Maghrebian Journal of Pure and Applied Science
ISSN : 2458-715X
http://revues.imist.ma/?journal=mjpas&page=index

(Z)-2-benzylidene-2H-[1,4]benzothiazin-3-one(T1)as New Synthesized Corrosion Inhibitor for Mild Steel in 0.5 M H_2SO_4

H. Elmsellem[1*],A. Elyoussfi[1], N. K.Sebbar[2], A. Dafali[1], K. Cherrak[1], H. Steli[3],E. M. Essassi[2], A. Aouniti[1]and B. Hammouti[1]

[1]URAC18, COST,Laboratoire de ChimieAppliquée et environnement, Department of Chemistry, Faculty of Sciences, Mohamed 1st University, P.O. Box 717, Oujda, 60000, Morocco.
[2]Laboratoire de Chimie Organique Hétérocyclique, URAC 21, Pôle de Compétences Pharmacochimie, Université Mohammed V, Faculté des Sciences, Av. Ibn Battouta, BP 1014 Rabat, Morocco.
[3]Laboratoire mécanique & énergétique, Faculté des Sciences, Université Mohammed Premier, Oujda, Morocco

**Corresponding author: h.elmsellem@yahoo.fr*
Received 14 Oct 2015, Revised 15 Nov 2015, Accepted 16 Nov 2015

Abstract:

The corrosion inhibition of mild steel in 0.5 M H_2SO_4 solution by (Z)-2-benzylidene-2H-[1,4]benzothiazin-3-one: (T1) has been studied using electrochemical polarization , electrochemical impedance spectroscopy (EIS) and weight loss methods. The corrosion inhibition efficiency measured by all the three techniques was in good agreement with each other. The results showed that T1 is a very good inhibitor for mild steel in acidic media. The inhibition efficiency increases with increasing inhibitor concentration. It acts as a mixed-type inhibitor. EIS plots indicated that the addition of T1 increases the charge-transfer resistance (R_{ct}), decreases the double-layer capacitance (C_{dl}) of the corrosion process, and hence increases inhibition efficiency. The adsorption of the T1 on the mild steel surface in acid solution obeys the Langmuir adsorption isotherm.

Keywords:[1,4]Benzothiazin-3-one, Mild steel, EIS, Corrosion, 0.5 H_2SO_4, DFT.

1. Introduction

The use of inhibitors is one of the most practical methods for protection against corrosion, especially in acidic media[1]. Among numerous inhibitors that have been tested and applied industrially as corrosion inhibitors. In our laboratory, many studies have been published on the use of products as corrosion inhibitors in acidic media[2].
In our present investigation, corrosion inhibition behavior of 2H-benzo[b][1,4]thiazin-3(4H)one(**T1**) in 0.5M H_2SO_4 for mild steel has been studied by gravimetric and electrochemical m ethods. hoice of this compound as corrosion inhibitor is based on the facts: benzo thiazin can be easi ly syn
hesized and it is highly soluble in studied medium. The higher solubiliy, and reactivity of benzo thiz

in is due to presence of group phenyl and electronegative heteratoms (S, O, N) groups present in 2 f acilitate the adsorption process [3].

2. Experimentalresults and discussion

2.1. Synthesis of Corrosion Inhibitors

- *Synthesis of(Z)-2-benzylidene-2H-[1,4]benzothiazin-3-one (T1)*

A solution of the 2*H*-[1,4]-benzothiazin-3-one (2.84mmol)in 10 ml of DMF was added sodium methoxide in excess and benzaldehyde (6.24 mmol). Under stirring, the mixture is led to reflux for 48 h. After filtration of the salts, the filtrate was concentrated under reduced pressure. The residue is purified on silica gel column and recrystallized with hexane. Yield 65%; (m.p.110-112K). The molecular structure of T1 is shown in scheme 1.

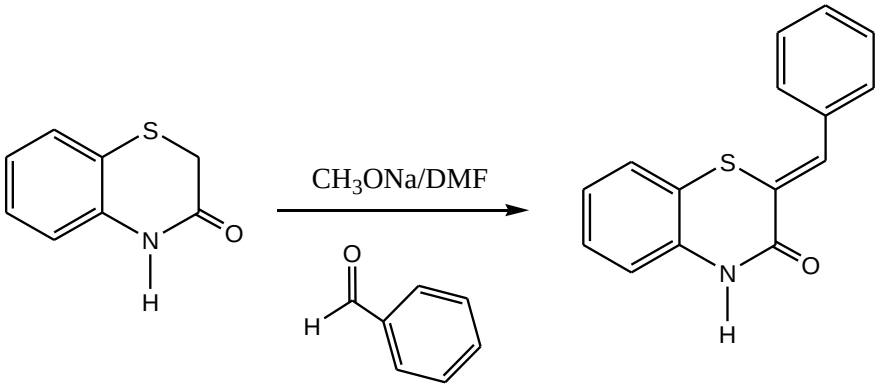

Scheme 1: Synthesis and characterization of (Z)-2-benzylidene-2H-[1,4]benzothiazin-3-one: **(T1)**.

The analytical and spectroscopic data are conforming to the structure of compound formed.(P1):Yield = 65%; M.p.110-112K; RMN1H (DMSO-d6) δ ppm : 6.99-7.66 (m, 9H, Har); 7.78(s, 1H; =CH-C6H5); 11.02(s, 1H; NH); RMN13C (DMSO-d6) δ ppm : 117.2, 123.7, 125.7, 127.5, 129.2, 129.2, 129.4, 130.3, 130.3, 131.2, (CHar); 115, 4, 120.8, 134.6, 134.7 (Cq), 159.1 (C=O).

1,4-benzothiazine and its derivatives constitute an important class of heterocyclic compounds which possess a wide range of therapeutic and pharmacological properties[4-7].

2.2. Material

Coupons were cut into 1.5× 1.5 × 0.05 cm^3 dimensions having composition (0.09%P, 0.01 % Al, 0.38 % Si, 0.05 % Mn, 0.21 % C, 0.05 % S and Fe balance) used for weight loss measurements. Prior to all measurements, the exposed area was mechanically abraded with 180, 400, 800, 1000, 1200 grades of emery papers. The specimens are washed thoroughly with bidistilled water degreased and dried with ethanol.

The aggressive solutions of 0.5M $H_2SO_4$was prepared by dilution of analytical grade 98% H_2SO_4 with distilled water. The concentration range of (T1) employed was 10^{-6}–10^{-3} M.

2.3.Gravimetric measurements

The gravimetric experiments were performed as described previously [8]. All experiments were triply performed and mean values were reported. Corrosion rate C_R (mg cm^{-2} h^{-1}) was calculated using following relation:

$$C_R = \frac{W}{At} \qquad (1)$$

Where *W* is the average weight loss of three parallel mild steel strips, *A* the exposed area of mild strip and *t* is immersion time (6h). From this calculated corrosion rate (C_R), the inhibition efficiency (η %) and surface coverage (θ) were calculated using following relationship:

$$\eta\% = \frac{C_R - C_{R(i)}}{C_R} \times 100 \quad (2)$$

$$\theta = \frac{C_R - C_{R(i)}}{C_R} \quad (3)$$

Where C_R and $C_{R(i)}$ are the corrosion rate values in absence and presence of T1 respectively.

2.4. Electrochemical measurements

The electrochemical study was carried out using a potentiostat PGZ100 piloted by Voltamastersoft-ware. This potentiostatis connected to a cell with three electrode thermostats with double wall. A saturated calomel electrode (SCE) and platinum electrode were used as reference and auxiliary electrodes, respectively. Anodic and cathodic potentiodynamic polarization curves were plotted at a polarization scan rate of 0.5mV/s. Before all experiments, the potential was stabilized at free potential during 30 min. The polarisation curves are obtained from −800 mV to −200 mV at 308 K. The solution test is there after de-aerated by bubbling nitrogen. The electrochemical impedance spectroscopy (EIS) measurements are carried out with the electrochemical system, which included a digital potentiostat model Voltalab PGZ100 computer at Ecorr after immersion in solution without bubbling. After the determination of steady-state current at a corrosion potential, sine wave voltage (10 mV) peak to peak, at frequencies between 100 kHz and 10 mHz are superimposed on the rest potential. Computer programs automatically controlled the measurements performed at rest potentials after 0.5 hour of exposure at 308 K. The impedance diagrams are given in the Nyquist representation. Experiments are repeated three times to ensure the reproducibility.

2.5. Quantum chemical calculations

For the theoretical study, complete geometry optimizations of the molecules were performed using the Density Functional Theory (DFT) with the Beck's three parameter exchange functional and the Lee–Yang–Parr non-local correlation functional (B3LYP) with 6-311G(d,p) basis set of atomic orbitals as implemented in Gaussian 09 program package [9]. Some electronic properties such as energy of the highest occupied molecular orbital (E_{HOMO}), energy of the lowest unoccupied molecular orbital (E_{LUMO}), energy gap (ΔE) between LUMO – HOMO and dipole moment. The optimized molecular structures and HOMO, LUMO surfaces were visualized using Gauss View [10].

3. RESULTS AND DISCUSSION

3.1. Gravimetric measurement

3.1.1. Effect of concentration

Corrosion inhibition efficiency (η%), corrosion rate (C_R) and corresponding surface coverage (θ) for mild steel sample in 0.5M H_2SO_4after 6h immersion time was evaluated using gravimetric measurements and is summarized in Table1. The variation of inhibition efficiency with different concentrations of T1is shown in Figure 1. Results obtained from gravimetric measurements reveals that inhibition efficiency and surface coverage increases with increasing T1 concentration. The maximum surface coverage occurs obtained at $10^{-3}M$. It is observed from Table 1, that corrosion rate is much lower in presence of T1 than in absence of T1[11].

The analysis of these results (Figure 1) shows clearly that the corrosion rate decreases (V (mg/h.cm^2) while the inhibition efficiency (η %) increases with increasing inhibitor concentration reaching a maximum value of 94 % at a concentration of 10^{-3}M. This behavior can be attributed to the increase of the surface covered θ (η %/100), and that due to the adsorption of T1 compounds on the surface of the metal, as the inhibitor

concentration increases. We can conclude that T1is a good corrosion inhibitor for mild steel in 0.5M H_2SO_4 solution.

Table 1. Corrosion rate and inhibition efficiency in the absence and presence of T1in 0.5 M H_2SO_4at 308K

Inhibitor	**Concentration** (M)	***v*** (mg.cm^{-2} h^{-1})	***η*** **(%)**	***θ***
H_2SO_4	**0.5**	1.450	--	--
T1	**10^{-3}**	0.080	**94**	0.94
	10^{-4}	0.142	90	0.90
	10^{-5}	0.440	70	0.70
	10^{-6}	0.635	56	0.56

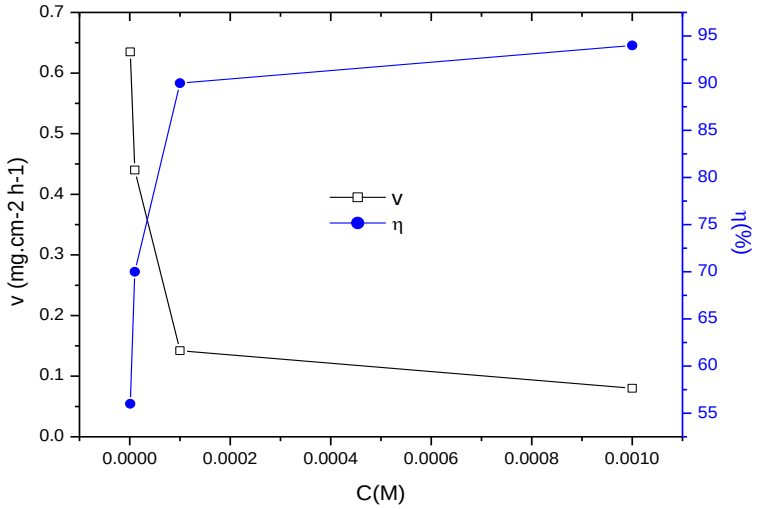

Figure 1. The corrosion rate and the inhibition efficiency for Mild steel in 0.5M H_2SO_4 containing different concentrations of T1.

3.1.2. Adsorption Isotherm

Mechanism of corrosion inhibition can be elucidated on the basis of molecular adsorption of T1 on metal surface [12]. Adsorption of inhibitors on metal surface depends on an assortment of factors such as chemical structure, temperature and electrochemical potential at metal/electrolyte interface. According to Quasi Lattice modal, surface of metals in aqueous solution of inhibitor is covered by water molecules.

Table 2: Values of $\Delta G°_{ads}$ of T1 for Mild Steel in 0.5M H_2SO_4.

Measurements	**Inhibitor**	**K_{ads} L mol^{-1}**	**$\Delta G°_{ads}$ kJ mol^{-1}**	**Linear coefficient regression (r)**
Weightloss	‘‘T1’’	325435.025	- 42.21	1.06096

Therefore, adsorption of T1 molecules takes place via subsequent replacement of water molecules with T1 as given below [13].

$$nH_2O_{(ads)} + T1_{(sol)} \Longrightarrow T1_{(ads)} + nH_2O_{(sol)}$$

where*n* is total number of water molecules replaced by one molecule of T1 from metal surface , commonly known as size ratio. It gives fundamental information about interaction between metal surface and T1. Various isotherms were tested but Langmuir adsorption isotherm (Figure2)was best fitted which can be expressed by the equation:

$$\frac{C_{(inh)}}{\theta} = \frac{1}{K_{(ads)}} + C_{(inh)} \qquad (4)$$

where$K_{ads}$is the equilibrium constant of the adsorption–desorption process,$\theta$is the degree of surface coverage and C_{inh} is molar concentration of T1. Adsorption constant related to standard energy of adsorption (ΔG°_{ads}) by the equation [14]:

$$K_{ads} = \frac{1}{55.5}\exp\left(\frac{-\Delta G^{\circ}_{ads}}{RT}\right) \qquad (5)$$

where R is gas constant, T is absolute temperature and 55.5 represent the concentration of water in acid solution (mol/dm^3). The value of standard free energy change (ΔG°_{ads}) at optimum concentration of T1is given in Table 2.From table, it is obvious that the value of ΔG°_{ads} are negative in presence of T1 which disclose that adsorption of T1 on metal surface is a spontaneous process and T1 form a strong film mild steel surface [15].Moreover, literature studied reveals that the value of $\Delta G^{\circ}_{ads,}$ -20 kJ/mol or less associated with electrostatic interaction between metal surface and charge inhibitor molecule i.e. physisorption and value of $\Delta G^{\circ}_{ads,}$ -40 kJ/mol or more negative related to the charge transfer from inhibitor molecule to the mild steel surface to form coordinate type of interaction i.e. chemisorption [16-18]. In our present case the value of $\Delta G^{\circ}_{ads}$is around -42.21 kJ /mol which suggest the chemisorption mode of adsorption of T1.

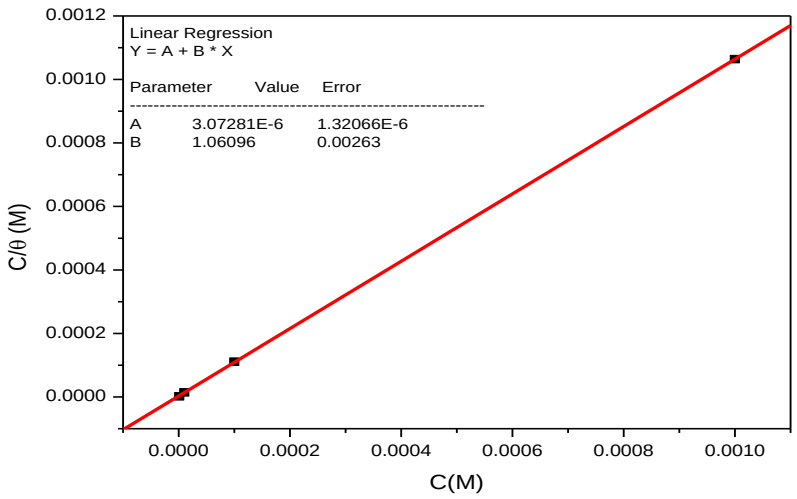

Figure2.Langmuir adsorption of **''T1''** on the mild steel in 0.5M H_2SO_4.

3.2. Electrochemical Measurements

3.2.1. Potentiodynamic polarization measurement

Figure 3 shows the polarization curves of mild steel in 0.5 M H2SO4 and in the presence of different concentrations (10^{-6} to 10^{-3} M) of T1. With the increase of T1 concentrations, both anodic and cathodic currents were inhibited. This result shows that the addition of T1 inhibitor reduces anodic dissolution and also retards the hydrogen evolution reaction.

The inhibition efficiencies were calculated from I_{corr} values according to following equation:

$$Ep\% = \frac{\text{icor}(0)-\text{icor}(\text{inh})}{\text{icor}(0)} \text{x } 100 \quad (6)$$

where*icor(0)*and *icor(inh)*are the corrosion current densities in the absence and the presence of the inhibitor.

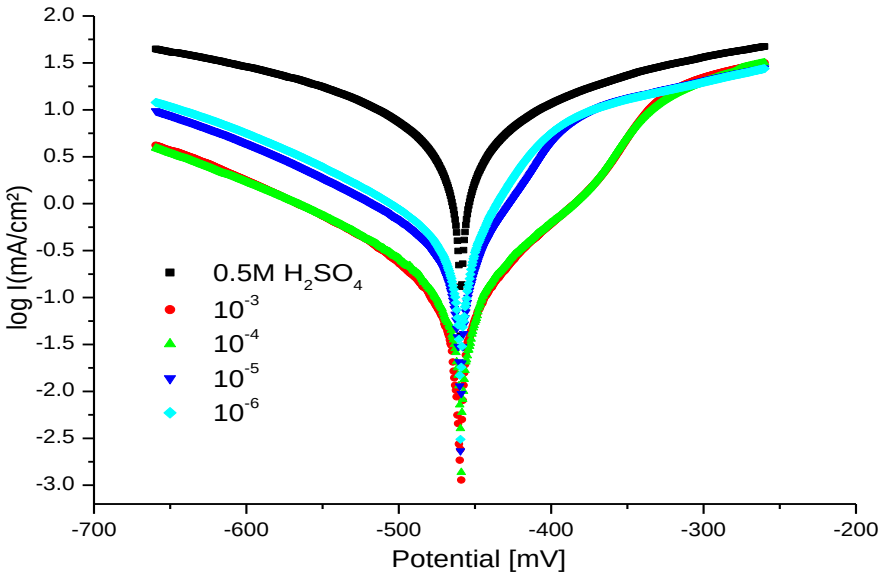

Figure 3. Potentiodynamic polarization curves of mild steel in 0.5M H_2SO_4 in the presence of different concentrations of T1.

Table 3 gives the values of corrosion kinetic parameters as the corrosion potential Ecorr , corrosion current density Icorr , cathodic Tafel slope (βc), and inhibition efficiency (Ep%) for the corrosion of mild steel in 0.5M H_2SO_4 with different concentrations of T1. The corrosion current densities were estimated by Tafel extrapolation of the cathodic curves to the open circuit corrosion potentials.

Table 3. Polarization parameters and corresponding inhibition efficiency for the corrosion of the mild steel in 0.5 M H_2SO_4without and with addition of various concentrations of (T1) at 308K.

Inhibitor	**Concentration** (M)	**E_{corr}** (mV/ECS)	**I_{corr}** (µA/cm²)	**$-\beta_c$** (mV/dec)	**Ep** (%)
H_2SO_4	**0.5**	-454	1975	190	--
T1	**10^{-3}**	-453	171	137	**91**
	10^{-4}	-458	181	144	90
	10^{-5}	-459	495	148	75
	10^{-6}	-455	643	149	67

These results revealed that the corrosion current density (Icorr) decreased remarkably with the increasing inhibitor concentrations, leading to the increase of inhibition efficiency.

A compound is usually classified as an anodic or a cathodic type inhibitor when the change in Ecorr value is larger than 85 mV [19-20]. Since the small displacement of the corrosion potential was about 5 mV (Table 3) after the addition of the T1, suggesting that the inhibitor acted as a mixed-type inhibitor. The values of the cathodic Tafel slopes, βc, were found to vary a range of 137-149 mV/dec. Therefore, the cathodic slope value was found to remain constant with increasing concentration of T1 in 0.5M H_2SO_4. Thus, the presence of the inhibitor does not affect the cathodic slopes (βc). This indicates that addition of T1 does not modify the mechanism of the proton discharge reaction. The values of inhibition efficiency (Ep %) increase with inhibitor concentration reaching a maximum value (91%) at 10^{-3} M.

3.2.2 Electrochemical impedance spectroscopic measurements

Nyquist plots of mild steel in 0.5 M H_2SO_4 in the presence and absence of additive are given in Figure 4. These curves were obtained after 30 min of immersion in the corresponding solution.

All the plots display a single capacitive loop. Impedance parameters derived from the Nyquist plots, percent inhibition efficiencies, E_{Rt} (%) and the equivalent circuit diagram are given in Table 4 and Figure 5, respectively.

The values of *R*t were given by subtracting the high frequency impedance from the low frequency one as follow [21]:

$$\mathbf{Rt=Zre}\text{(at a low frequency)}\mathbf{- Zre}\text{(at a higt frequency)} \quad (7)$$

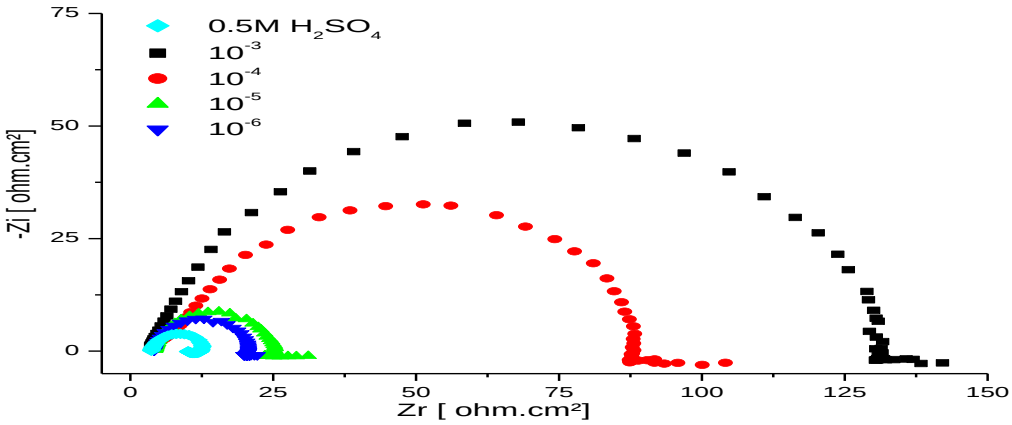

Figure 4. Nyquist diagrams for mild steel electrode with and without T1 at E_{corr} after 30min of immersion.

The values of electrochemical double layer capacitance, *C*dlwere calculated at the frequency *f*max, at which the imaginary component of the impedance is maximal (-Zmax) by the following equation [22]:

$$\boldsymbol{C_{dl}= 1/2\pi f_{max}R_t} \quad (8)$$

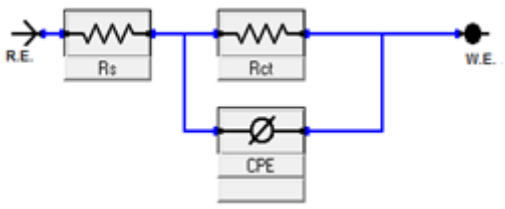

Figure 5. The electrochemical equivalent circuit used to fit the impedance spectra

The depressed capacitive loop in Nyquist plot at high frequency region may be attributed due to charge transfer reaction between metal and T1, formation of electrical double layer and surface inhomogeneity [23, 24]. The impedance *CPE* was calculated using following formula:

$$Z_{CPE} = Q^{-1}(j\omega)^{-n} \quad (9)$$

Where *Q* is *CPE* coefficient, *n* is *CPE* exponent, ω is the angular frequency($\omega = 2\pi f$, where *f* is AC frequency). For CPE to behave like an ideal capacitance (C_{dl}), value of *n* should be one [25].

The percent inhibition efficiency (E_{Rt}) is calculated by charge transfer resistance obtained from Nyquist plots, according to the equation:

$$E=(1-R^{\circ}_{ct}/ R_{ct})x100 \qquad (10)$$

In this equation, R_{ct} and R°_{ct} are the charge transfer resistance with and without the T1, respectively.

Table 4. Impedance parameters of mild steel in 0.5M H_2SO_4 containing different concentrations of T1.

Inhibitor	Concentration (M)	R_{ct} (Ω cm^2)	C_{dl} (µf/cm^2)	E (%)
H_2SO_4	**0.5**	12	134	--
T1	**10^{-3}**	129	30.19	**91**
	10^{-4}	83	30.70	86
	10^{-5}	21	94.00	43
	10^{-6}	16	124.00	25

As can be seen from this table the increase in resistance in the presence of T1, compared to H_2SO_4, alone is related to the corrosion inhibition effect of the molecules. The value of C_{dl} decreases in the presence of this inhibitor. The decrease in C_{dl}, which can result from a decrease in local dielectric constant and/or an increase in the thickness of the electric double layer [26, 27], suggested that T1 molecules function by adsorption at the metal/solution interface. Thus, the decrease in C_{dl} values and the increase in R_{ct} values and consequently of inhibition efficiency may be due to the gradual replacement of water molecules by the adsorption of the T1 molecules on the metal surface, decreasing the extent of dissolution reaction [28, 29].
The results obtained by this method are in good agreement with the values of inhibitor efficiency obtained from weight loss and polarization measurements.

4. Quantum chemical studies

The effectiveness of an inhibitor can be related to its spatial molecular structure, as well as with their molecular electronic structure [30, 31]. Inhibitor efficiency depends on the structure and the chemical properties of the inhibitor being adsorbed.

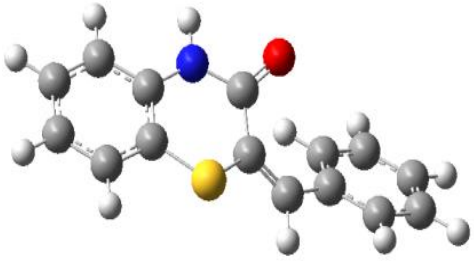

Figure 6. Optimized Structure of T1

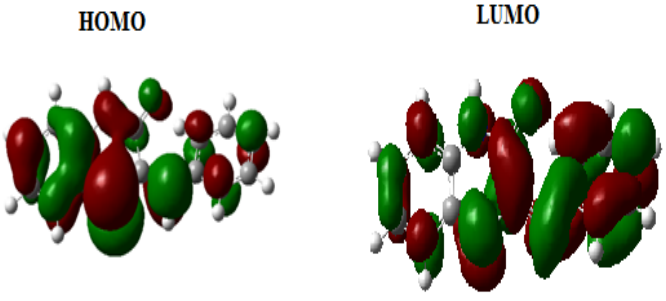

Figure.7. The frontier molecular orbital density distribution of T1.

The values E_{HOMO}, E_{LUMO} and dipole moment (μ) were derived from geometricallyoptimized T1molecule (Figure 6). Figure 7 represent the HOMO and LUMO frontier molecular orbital diagrams of the T1, respectively. From the calculated values of E_{HOMO}, E_{LUMO} the value of ΔE are calculated and given in Table 5. A very high value of E_{HOMO} (-0.283) and small value of E_{LUMO} (-0.206) suggestthat T1 has strong tendency to transfer its electrons to the appropriate empty d-orbitals of thesurface atoms as well as to accept the electrons from the d-orbitals of the Fe-atoms in to its piantibondingmolecular orbitals [32]. Moreover, the value ofdipole moment (μ) is much higher (2.0382Debye) as compare to the $\mu$of water (1.85 Debye)suggesting that T1 has much stronger tendency to adsorb on the mild steel surface inaqueous acidic solution[33].

Table 5. Quantum chemical parameters of T1.

Quantum parameters	T1
$\mathbf{E_{HOMO}}$ (eV)	-0.283
$\mathbf{E_{LUMO}}$ (eV)	-0.206
μ (debye)	2.0382

5. CONCLUSION

From the experimental and theoretical results it is concluded that investigated inhibitor acts as good corrosion inhibitor for mild steel in 0.5 M H_2SO_4 . Its inhibition efficiency increases with increasing concentration and maximum efficiency was obtained at 10-3M concentration. EIS results suggested that T1 form surface film at metal/ electrolyte interface. Tafel polarization study shows that T1 acts as mixed type inhibitor. The quantum chemical calculations well supported the experimental results and also show that T1 has strong tendency to replace the water from metal surface.

REFERENCES

1. H. Elmsellem, H. Bendaha, A. Aouniti, A. Chetouani, M. Mimouni, A. Bouyanzer. Mor. **J. Chem. 2 (1),1-9 (2014).**
2. I. El Mounsi, H. Elmsellem, A. Aouniti, H. Bendaha, M. Mimouni, T. Benhadda, R. Mouhoub, B. El Mahi, A. Salhi and B. Hammouti. **Der Pharma Chemica, 7(10):350-356 (2015).**
3. H. Elmsellem, M. H.Youssouf, A. Aouniti, T. Ben Hadd, A. Chetouani, B. Hammouti. Russian, **Journal of AppliedChemistry. 87(6), 744−753 (2014).**
4. N. K. Sebbar, A.Zerzouf, E. M. Essassi, M. Saadi&L. El Ammari, Acta Cryst,2014a, E70, o160–o161.
5. J. Gowda.,. A.M.A. Khader., B. Kalluraya., P. Shree., A.R. Shabaraya. **European Journal of Medicinal Chemistry.46, 4100- 4106 (2011).**
6. N. K. Sebbar, A. Zerzouf, E. M. Essassi, M. Saadi.,L. El Ammari. **Acta Cryst, b, E70, o116 (2014).**
7. N. K. Sebbar, A. Zerzouf, E. M. Essassi, M. Saadi&L. El Ammari. **Acta Cryst, c, E70, o614 (2014).**
8. A. Elyoussfi, H. Elmsellem, A. Dafali, K. Cherrak, N. K. Sebbar, A. Zarrouk, E. M. Essassi, A. Aouniti, B. El Mahi and B. Hammouti. Der Pharma Chemica.7(10), 284-291 (2015).
9. H. Elmsellem, N. Basbas, A. Chetouani, A. Aouniti, S. Radi, M. Messali, B. Hammouti**. PortugaliaeElectrochimicaActa, 32(2), 77-108 (2014).**
10. H. Elmsellem, A. Aouniti, M. Khoutoul, A. Chetouani, B. Hammouti, N. Benchat, R.Touzani and M. Elazzouzi. **Journal of Chemical and Pharmaceutical Research. 6(4), 1216-1224 (2014).**
11. N. K. Sebbar, H. Elmsellem, M. Ellouz, S. Lahmidi, E. M. Essassi, I. Fichtali, M. Ramdani, A. Aouniti, A. Brahimi and B. Hammouti. **Der Pharma Chemica.7(9), 33-42 (2015).**
12. H. Elmsellem H., A. Aouniti, M.H .Youssoufi, H. Bendaha, T. Ben hadda, A.Chetouani, I. Warad, B. Hammouti, **Phys. Chem. News.70, 84 (2013).**
13. B.S. Sanatkumar, J. Nayak, A.N. Shetty, **Int. J. Hydrogen Energy. 37, 9431 (2012).**

14. M. Abdallach, **Corros. Sci, 44 ,717 (2002).**
15. H. Elmsellem, A. Aouniti, Y. Toubi, H. Steli, M. Elazzouzi, S. Radi, B. Elmahi, Y. El Ouadi, A. Chetouani, B.Hammouti. **Der Pharma Chemica. 7(7), 353-364 (2015).**
16. Z. S. Smialowska, J. Mankowski, Corros. Sci.18, 953(1978).
17. A.Yurt, S. Ulutas, H. Dat,.**Appl. Surf. Sci.253, 919 (2006).**
18. N. K. Sebbar, H. Elmsellem,M. Ellouz, S. Lahmidi, A.L. Essaghouani, E. M. Essassi,M. Ramdani, A. Aouniti1, B. El Mahi and B. Hammouti. **Der Pharma Chemica. 7(10), 579-587 (2015).**
19. A.Y Musa, A.A.H. Kadhum, A. B. Mohamad, M.S. Takriff, **Corros. Sci, 52, 3331(2010)..**
20. J. Zhang, X. L. Gong, H. H .Yu, M. Du,.**Corros. Sci.53,332(2011).**
21. Q. B. Zhang, Y. X Hua, **Acta, 2009, 54,(1881).**
22. C. Das,.**Indian Journal of Chemical Technology,. 3(5), 259(1996).**
23. H. Elmsellem, K. Karrouchi, A. Aouniti, B. Hammouti, S. Radi, J. Taoufik, M. Ansar, M. Dahmani,H. Steli and B. El Mahi. **Der Pharma Chemica,.7(10), 237-245 (2015).**
24. S.L.A. Kumar, M. Gopiraman, M. S. Kumar, A. Sreekanth, Ind. Eng.Chem. Res, 2011, 50,7824.
25. C. Verma, A. Singh, G. Pallikonda, M. Chakravarty, M.A. Quraishi, I. Bahadur, E.E. Ebenso, **J. Mol. Liq.209, 306 (2015).**
26. A. H. Al. Hamzi, H. Zarrok, A. Zarrouk, R. Salghi, B. Hammouti, M. Bouachrine, A. Amine, H. Oudda, Der Pharmacia Lettre,2013, 5(2), 27.
27. E. H. McCafferty, N. Ackerman,.**J. Electrochem. Soc.119, 146(1972).**
28. F. Bentiss, M Traisnel, M. Lagrenée, **Corros. Sci., 42, 127(2000).**
29. S. Muralidharan, K. L .N. Phani, S. Pitchumani, S. Ravichhandran, S. V. K. Iyer**, J. Electrochem. Soc,,142,1478 (1995).**
30. H. Elmsellem, T. Harit, A. Aouniti, F. Malek, A. Riahi, A. Chetouani , and B. Hammouti. **Protection of Metals and Physical Chemistry of Surfaces, , 51(5), 873–884 (2015).**
31. H. Elmsellem, H. Nacer, F. Halaimia, A. Aouniti, I. Lakehal, A .Chetouani, S. S. Al-Deyab, I. Warad, R. Touzani, B. Hammouti. **Int. J. Electrochem. Sci. 9, 5328 – 5351 (2014).**
32. S. Banerjee, Mishra, A., Singh, M.M., Maiti, B., Ray, B., Maiti, P., Maiti, B., Ray, B., Maiti, P.,**RSC. Adv.1, 199-205 (2011).**
33. Y.M. Tang, W.Z. Yang, X.S. Yin, Y. Liu, R. Wan, J.T. Wang, **Mater. Chem. Phys.116, 479-483 (2009).**

(2015) ;http://revues.imist.ma/?journal=mjpas&page=index